



Published in final edited form as:

Pediatr Res. 2011 August ; 70(2): 159–165. doi:10.1203/PDR.0b013e3182218622.

Chronic hypoxia impairs murine hippocampal development and depletes the postnatal progenitor pool by attenuating mTOR signaling

Lakshmi Raman, Xiangmei Kong, Jennifer A. Gilley, and Steven G. Kernie

Departments of Pediatrics and Developmental Biology, University of Texas Southwestern Medical Center, Dallas, TX 75390

Abstract

Chronic hypoxia (CH) is a major risk factor for impaired cognitive function in various disease states, particularly in the context of cyanotic congenital heart disease. While most brain development occurs prenatally, the dentate gyrus (DG) of the hippocampus harbors progenitor stem cells that contribute to its ongoing development postnatally. It is unclear how exposure to CH might affect postnatal hippocampal development, so we utilized a transgenic mouse that expresses enhanced green fluorescent protein (eGFP) within this progenitor population to determine the effect of CH on the DG. We find that exposure to 10% oxygen from postnatal day 3 to 28, results in a smaller DG with long-term impairment of hippocampal neurogenesis. Since the mammalian target of rapamycin (mTOR) pathway is a well-known regulator of cell proliferation and growth and is sensitive to hypoxia, we investigated its activation upon exposure to CH and find it to be attenuated specifically in neural progenitor cells. Systemic inhibition of the mTOR pathway using rapamycin also caused impairment of hippocampal neurogenesis that mimics exposure to CH. Our findings demonstrate that CH results in long-term impairment of hippocampal neurogenesis and is mediated, in part, by attenuation of the mTOR pathway.

Introduction

Many infants with cyanotic heart disease are in a state of chronic hypoxia (CH) for the first 2 to 3 years of life prior to repair of the cardiac lesion. CH that begins in these infants at birth occurs during critical time points of hippocampal development (1). Using a rodent model of CH we have previously shown a significant alteration in the hippocampal neurometabolome (2) and dendritic arborization in the hippocampus (3). Given the significant alterations in the hippocampus in CH we investigated how dentate gyrus (DG) neurogenesis, which occurs primarily postnatally, might also be affected. The DG in the hippocampus is one of two well-characterized areas where neurogenesis is known to persist throughout life (4). This region has stem/progenitor cells that are the source of the DG granular neurons (5, 6).

Copyright © 2011 International Pediatric Research Foundation, Inc. All rights reserved.

Corresponding Author: Lakshmi Raman, M.D., Departments of Pediatrics and Developmental Biology, UT Southwestern Medical Center at Dallas, 5323 Harry Hines Blvd, Dallas, TX 75390, Phone: 214-648-1242, Fax: 214-648-1960, Lakshmi.Raman@UTSouthwestern.edu.

Publisher's Disclaimer: *Pediatric Research Articles Ahead of Print* contains articles in unedited manuscript form that have been peer-reviewed and accepted for publication. As a service to our readers, we are providing this early version of the manuscript. The manuscript will undergo copyediting, typesetting and review of the resulting proof before it is published in its final definitive form. Please note that during the production process errors may be discovered, which could affect the content, and all legal disclaimers that apply to the journal pertain.

The neural stem and progenitor cells in the subgranular layer of the DG have been classified using a neural progenitor-specific nestin-GFP expressing transgenic mouse as type 1, 2a, 2b and 3 cells (7, 8). The early stem/progenitors (type 1 and 2a) express the neuroepithelial marker nestin while the late progenitors (type 2b and 3) downregulate the expression of nestin and begin to express markers of developing neurons such as the microtubule protein doublecortin (DCX) and polysialated neural cell adhesion molecule (PSA-NCAM) (8). These cells are stimulated in response to environmental enrichment as well as various other physiological stimuli (9). There is also evidence to suggest that subsets of these progenitor cells are vulnerable to external insults such as hypoxia-ischemia and trauma (10, 11).

We wanted to study the effects of CH on the progenitor stem cell population in the hippocampus and the underlying mechanism involved. To investigate the underlying mechanism of the effects of CH on neurogenesis, we examined the role of the mammalian target of rapamycin (mTOR) pathway, as hypoxia is an important regulator of the mTOR pathway. Under acute hypoxic conditions, cells regulate the limited energy available by inhibiting energy intensive processes such as protein translation (12). The inhibition of mTOR, a protein that is required for proper cell proliferation and growth, is the major mechanism through which this is achieved (13). The mTOR pathway plays critical roles in proper brain development including axonal guidance, dendritic development, and dendritic morphogenesis (14, 15). mTOR has also been implicated in neurodegenerative disorders such as Alzheimers, Huntingtons and Parkinsons diseases (16–18). We hypothesized that CH would decrease the progenitor stem pool in the DG of the hippocampus and that this may be mediated through impairment of mTOR signaling.

Methods

Animal preparation

The study was approved and conducted according to the guidelines of the Institutional Animal Care and Use Committee at the University of Texas Southwestern Medical Center. The animals were housed and cared for in the Animal Resource Center (ARC) at UT Southwestern Medical Center in compliance with standards for humane and compassionate use of animals in biomedical research. Transgenic mice expressing GFP under the control of the nestin promoter and second intron (nestin-GFP) that were previously generated in our lab were back-crossed into the CD1 background for eight generations (19). Offspring were genotyped using the previously published protocol. Nestin-GFP transgenic CD1 mice were used for all experiments. Animals are housed with a 12:12 hour dark and light cycle with free access to food and water.

Induction of Chronic Hypoxia

Dams and their pups were randomly assigned to control or CH groups. The dams and their pups in the CH group were housed in a plexiglass chamber (oxygen concentration 10% \pm 0.1%) from postnatal day (P) 3 until day 7, 14 and 28. For P56 experiments, animals in the CH group were placed in the chamber from P3 to P28 and then in normoxia until day 56. Details outlined in reference (2). The pups in the CH had less body weight by about 40% at P7,14 and 28. We have previously demonstrated that the brain weight in this model is reduced in the CH group (2).

5-Bromo-2-deoxyuridine (BrdU) injection

To determine the proliferation profile of the progenitor stem cell population, a single dose of BrdU (50mg/kg) (Sigma-Aldrich, St. Louis, MO) dissolved in sterile water was given intraperitoneally (i.p.) 2 hours prior to sacrifice on P7, P14, P28 and P56. This dose captures most of the proliferating cells particularly as these are young animals. To capture the long-

term fate of the progenitor stem pool, a separate set of animals in the control and CH group received a single BrdU injection (50mg/kg) given i.p. on P28, and were sacrificed on P56.

Rapamycin injection

To examine the role of pharmacological inhibition of the mTOR pathway on neurogenesis, a separate cohort of animals were given daily injections of rapamycin (LC laboratories, Boston, MA) starting from P5 until P9 at a dose of 50 µg/kg and from P10 to P14 at a dose of 100 µg/kg i.p. Animals were given BrdU (50mg/kg) i.p. 2 hours prior to sacrifice.

Immunohistochemistry (IHC)

IHC was performed as outlined in reference (20). A DAB protocol was used for stereology measurements and double-labeling immunofluorescence was used to obtain images that are shown. To measure volume, sections obtained from the entire hippocampus were stained with Nissl staining and volume was measured using MetaView analysis at P14 and P56.

Cell Quantification

Unbiased estimates for volume and cell counts were obtained using stereological quantification on an Olympus BX51 System Microscope with a MicroFIRE A/R camera (Optronics). An unbiased counting frame was used with the help of the Optical Fractionator Probe within the Stereo Investigator software. For GFP and DCX cell counting, a 100x, 1.4 NA oil immersion lens was used and for BrdU cell counting a 40x, 0.75 NA lens was used. A minimum of 350 cells per animal was counted. The average number of sections was 8 to 10 per animal and average thickness of the section after processing was approximately 30 µm. The optical dissector height was 24 µm with 3 µm guard zone on either side. For counting frame size please refer to the table.

In order to reduce bias between samples a number of precautions were taken. All samples were processed in a similar manner. To provide room for shrinkage of tissues after processing, average mounting thickness of 30 µm was used. Every 6th section was used for counting and only animals where all the sections were present were used for quantification. The average Schaffer coefficient of error for each staining and time point is mentioned in table 1. Images shown were obtained by Zeiss LSM 510 confocal microscope utilizing Argon 488 and He 633 lasers.

Western Blot

Cortex was dissected out in both the control and CH groups at P14, homogenized. 20 µg of protein was loaded on 12% SDS-PAGE (sodium dodecyl sulfate-polyacrylamide gel electrophoresis) for p70 ribosomal S6 protein kinase (S-6) and total S-6 kinase blot and 10% SDS-PAGE for total and phosphorylated elf-4E binding protein (4E-BP1) blot. Antibodies used included rabbit anti-phospho-S-6, total S-6 (cell signaling) at 1:1000, rabbit anti-phospho 4E-BP1 and total 4E-BP1 (cell signaling) at 1:1000 and rabbit anti β-tubulin (sigma) at 1:30,000. All secondary antibodies were raised in goat serum (Santa Cruz) and used in dilution of 1:10,000.

Protein concentrations were measured (BCA protein assay kit), gels were run and protein transferred to a PVDF membrane. After membranes were blocked with 4% BSA for one hour they were incubated with primary antibody overnight at 4°C followed by secondary antibody for 2 hours at room temperature. Membranes were washed with PBS-1% Tween. Protein bands were visualized and quantified by densitometry analysis using Kodak Molecular Imaging Software 4.0.3 and the quantity adjusted to the total protein and anti-β-tubulin density.

Real-time PCR

Dentate gyrus was microdissected from the hippocampus on P14 in both control and CH groups. Cell sorting and RNA extraction was done as outlined in reference (20). The primer sequence is as follows. GAPDH forward: 5'-CTC AAC TAC ATG GTC TAC ATG TTC CA-3'; GAPDH reverse 5'-CCA TTC TCG GOC TTG ACT GT-3'; S6 forward: 5'-TCG GCT GTG TCA AGA TGA AG-3'; S6 reverse 5' CAT GGA AAA ACC TTG CTT GT-3'. Real time quantification was analyzed on the Applied Biosystems 7,500 Real-time PCR system software.

Statistics

Unpaired t-test with unequal variance was used to compare the effect of CH on progenitor stem cell population at each time point. Paired t-test with equal variance was used to compare the effect of CH on the mTOR pathway by western and real time PCR. The data are presented as mean \pm SD and statistical significance was set at $p < 0.05$.

Results

Chronic Hypoxia Decreases the Progenitor Pool

To quantify the progenitor stem cell population within the DG, design-based stereology was used to estimate the number of early progenitors (GFP-expressing cells) and actively dividing (BrdU-expressing) cells in *nestin-GFP* transgenic mice at postnatal day (P) 7, 14 and 28. Late progenitors of the DG were estimated similarly at P14 by quantifying doublecortin (DCX)-expressing cells.

Following 4 days of hypoxic exposure (10% oxygen from P3–P7), mice were given one dose of BrdU to see how overall proliferation was affected. We observed that BrdU-expressing cells within the DG were reduced by approximately 50% ($14,240 \pm 3276$) when compared to normoxic controls ($24,109 \pm 3871$) (Fig. 1-C, D and T). To then determine whether these dividing cells were stem/progenitors that express GFP, we performed stereological counts and found that progenitors within the dentate were reduced similarly by almost 40% in the CH-exposed group ($34,562 \pm 1389$) compared to the control ($48,789 \pm 1424$) (Fig. 1A, B, and S).

To determine how CH-induced changes in proliferation progressed over time, we studied animals at P14 and at P28. Here, proliferation as evidenced by BrdU incorporation was also decreased, though not as dramatically as what was observed at P7. Overall proliferation was decreased by approximately 15% at P14 (8554 ± 667 in control vs 7361 ± 783 in CH) (Fig. 1-I, J, and T) and at P28 (2398 ± 254 in control vs 2043 ± 138 in CH) (Fig 1-O, P and T). GFP-expressing progenitors were also decreased by approximately 20% at P14 ($43,965 \pm 1365$ in control vs $35,793 \pm 1662$ in CH) (Fig 1-G, H and S) and 30% at P 28 ($42,198 \pm 4598$ in control vs $29,254 \pm 943$ in CH) (Fig 1-M, N and S) which was more pronounced than the decrease seen at P14. This is in marked contrast to the 40% reduction seen at P7.

Chronic Hypoxia Impairs Dentate Gyrus Development

Since CH impairs overall proliferation and decreases the number of GFP-expressing progenitors at all time points examined (Fig 1–B, H, N and S), we next wanted to determine whether the DG itself developed aberrantly. To determine this, we measured the volume of the neuronal layer of the DG at P14. We observed that the volume of the DG was significantly decreased by approximately 20% ($6 \pm 2.6 \times 10^8 \mu\text{M}$ in control vs $4.7 \pm 0.2 \times 10^8 \mu\text{M}$ in CH) (Fig. 2, A–D, G) in the CH group, which correlates well with the 20% reduction of proliferation observed at that time point (Fig 1- I, J and T).

We also wanted to determine whether this overall loss in neuronal volume could be explained by fewer late progenitors as labeled by DCX expression. Using unbiased stereology, we determined that DCX-expressing late progenitors at P14 were decreased by about 22% ($64,316 \pm 7801$ in control vs $50,084 \pm 7854$ in CH) (Fig. 2, E, F, and H.). Again, this correlates well with the overall decrease in the DG volume that is observed at this time point.

Recovery of Dentate Gyrus Volume Occurs Following 4 Weeks of Normoxia but Proliferation Remains Impaired

Immediately following exposure to CH, mice demonstrated stunted growth that normalized following exposure to normoxia. In order to determine whether a similar recovery occurs in the DG, we quantified the number of early progenitors (GFP- expressing) at P56 and found that these numbers had normalized after the animals had been in normoxia for 4 weeks ($27,720 \pm 2781$ in control vs $25,752 \pm 3345$ in CH) Similarly, when the DG volume was measured at P56, the group exposed to hypoxia from P3-P28 normalized its DG volume compared to normoxic controls ($5.2 \pm 0.42 \times 10^8 \mu\text{M}$ in control vs $5.2 \pm 0.12 \times 10^8 \mu\text{M}$ in CH). Figure 3 demonstrates that immediately following exposure to normoxia at P28, there was a rebound of BrdU-expressing cells within the DG (1710 ± 162 in control vs 2146 ± 215 in CH) (Fig. 3, A, B, and E). However, when mice exposed to hypoxia from P3-P28 were analyzed for proliferation at P56 by BrdU given just prior to sacrifice, there was a marked attenuation of proliferating cells in the mature DG (2103 ± 248 in control vs 1393 ± 161 in CH) (Fig 3, C, D and F). This suggests long-term impairment of the proliferative potential in the adult.

The mTOR Pathway is Impaired in Chronic Hypoxia

The mechanisms underlying CH –dependent attenuation of progenitors remain unclear but may involve mTOR. Two substrates in the mTOR pathway are S6 and 4E-BP1, which undergo mTOR-mediated phosphorylation and are used as readouts for pathway activation (13). We performed Western blot analysis on isolated cortex from hypoxia-exposed animals and determined that both phospho-S6 and phospho-4E-BP1 levels were attenuated in the cortex (Fig. 4, A-F). In order to determine the cell specificity of this effect, we utilized fluorescent activated cell-sorting (FACS) to isolate GFP-expressing progenitors from the DG of both control and CH-exposed mice. We quantified S6 mRNA levels in GFP-positive cells using quantitative PCR and found that mRNA expression is reduced by almost 50% in the CH group at both P7 and P14, and persists at P28 (Fig. 4, G). These data suggest that the mTOR pathway may be involved in the pathology of the aberrant hippocampal development that accompanies CH and that its attenuation is specific to the progenitor population.

mTOR Inhibition by Rapamycin Decreases the Progenitor Stem Cell Pool

We next investigated whether pharmacologically inhibiting the mTOR pathway using rapamycin phenocopies CH. Nestin-GFP animals were injected with rapamycin from P5 to P14 and sacrificed 2 hours following an injection of BrdU. Using unbiased stereology we quantified GFP-expressing early progenitors, DCX-expressing late progenitors and the actively dividing cells by BrdU incorporation on P14. Animals treated with rapamycin had significantly decreased numbers of both early and late progenitors as well as actively dividing cells compared to the control animals. These differences were similar to the changes observed in CH (Fig. 5, A–K). The decrease in GFP-expressing early progenitors, as quantified by the number of GFP-positive cells was 25% ($43,965 \pm 1365$ in control vs 33026 ± 1196 in rapamycin treated), while in DCX-expressing late progenitors it was 30% (64316 ± 7801 in control vs 44415 ± 5072 in rapamycin treated) whereas in BrdU-expressing actively dividing cells it was reduced by 45% (8554 ± 667 in control vs $4764 \pm$

369 in rapamycin treated). The percentage decrease is greater than that seen in animals exposed to CH at a similar time point.

Discussion

CH is an important risk factor for infants with cyanotic congenital heart disease and brain injury is a major cause of their neurological morbidity in these infants (21). The animal model of CH used in this study closely mimics the degree of hypoxia seen in infants with cyanotic heart disease (2) and has been widely used to study the effects of CH on the developing brain such as alteration in NMDA receptor expression and function, and alterations in energy metabolism (2, 22). Despite the clear association between CH and brain dysfunction, mechanisms underlying these observations remain unclear.

Here, we demonstrate a significant decrease in neurogenesis in the DG in mice exposed to CH. The DG is one of the two most well-characterized areas where neurogenesis occurs postnatally (4). The peak of DG neurogenesis occurs in mice, a time when the developing brain may be particularly sensitive to insults such as hypoxia (23). It is well known that the microenvironment affects the proliferative potential of a variety of organ-specific stem/progenitor cells (24). This may explain the almost 50% reduction in the progenitor stem cell population in the chronic hypoxic group at P7 when the microenvironment of the neurogenic niche is altered at the peak of its proliferative potential. The differentiation potential of the progenitor population suggests that at P7, most of the progenitors differentiate into neurons (20). Therefore, our observations demonstrating significant decreases in the neuronal pool of the developing DG under CH during this time are not unexpected. This is further confirmed by the decrease in the DCX-expressing late progenitor cell population and a decrease in the volume of the neuronal layer at P14 in CH. Altering the microenvironment during this phase of rapid development causes long-term impairment in the proliferative potential as evidenced by a decrease in the number of actively dividing cells at P56. This decrease seen at P56 suggest long-lasting impairment of proliferative potential or may represent just a lag in proliferation from the catch up growth seen when animals are removed from CH. The long-term effect of this change remains unknown.

To gain insight into one of the potential mechanisms underlying our observations, we examined the status of the mTOR signaling pathway. In the nervous system, mTOR has been implicated in axonal and dendritic development as well as pruning of dendritic arborizations (14, 15), which we have previously shown to be altered during exposure to CH (3). In cultured hippocampal neurons, 4E-BP1 is present in the dendrites and at synaptic sites (25). The mTOR pathway is a key regulator of cell growth and proliferation and has been implicated in neurogenesis and differentiation of progenitor stem cells (26). In a model of global ischemia, neurogenesis is induced through CD95 and its receptor CD95L (27), a process known to be mediated through activation of the mTOR pathway.

Since hypoxia is a major regulator of the mTOR pathway, we quantified levels of total and phosphorylated S6 and 4E-BP1 as readouts of mTOR activity, and demonstrated that phosphorylated levels of both are decreased in the cortex in CH. The significant decrease in the phosphorylation levels of both substrates in the cortex suggests that inhibition of mTOR activity may be an adaptive mechanism to limit energy expenditure. This is supported by a decrease in creatine levels and altered phosphocreatine to creatine ratio seen by proton spectroscopy in our model (2).

Finally, using rapamycin as a specific inhibitor of the mTOR pathway, we demonstrated a significant decrease in the early and late progenitors as well as the actively dividing cells seen in CH. Rapamycin has been shown to decrease neurogenesis and subsequent mossy

fiber sprouting in an adult mouse model of kainic acid-induced seizures (28). This model of seizure activity has been shown to be regulated by mTOR activation. Also, rapamycin has been used to decrease mTOR-induced neuronal differentiation of progenitor stem cells induced by insulin (26). Thus, it appears that the overall decrease in the progenitor stem pool in CH is mediated at least in part through mTOR signaling.

In conclusion we have demonstrated that CH causes a significant decrease in the progenitor stem pool and that this decrease may in part be mediated through mTOR signaling. Progenitor stem cells in the developing brain continuously add to the pool of functional neurons and other cell types throughout life (29). Such integration into the functional pool is likely critical for proper cognitive function, particularly early in hippocampal development. It has been shown that following other forms of injury such as traumatic brain injury and hypoxia-ischemia, there is an increase in the progenitor pool that helps replace the loss of functional neurons (10, 11). However, in CH, the long-term decrease in this progenitor pool may put the developing brain at greater risk for learning disorders later in life.

Acknowledgments

Statement of financial support: This study was supported by the Perot Family Center for Brain and Nerve Injuries at Children's Medical Center Dallas [L.R.] and NIH grant R01 NS048192 [S.G.K.].

We thank Gui Zhang for technical assistance, Dr. Raghu Rao for critical review and Dr. Renee McKay for manuscript preparation.

Abbreviations

BrdU	5-Bromo-2-deoxyuridine
CH	Chronic hypoxia
DG	Dentate gyrus
DCX	Double cortin
4E-BP1	Eukaryotic translation initiation factor
GFP	Green fluorescent protein
mTOR	Mammalian target of rapamycin

References

1. Avishai-Eliner S, Brunson KL, Sandman CA, Baram TZ. Stressed-out, or in (utero)? Trends Neurosci. 2002; 25:518–524. [PubMed: 12220880]
2. Raman L, Tkac I, Ennis K, Georgieff MK, Gruetter R, Rao R. In vivo effect of chronic hypoxia on the neurochemical profile of the developing rat hippocampus. Brain Res Dev Brain Res. 2005; 156:202–209.
3. Raman L, Hamilton KL, Gewirtz JC, Rao R. Effects of chronic hypoxia in developing rats on dendritic morphology of the CA1 subarea of the hippocampus and on fear-potentiated startle. Brain Res. 2008; 1190:167–174. [PubMed: 18083146]
4. Altman J, Das GD. Autoradiographic and histological evidence of postnatal hippocampal neurogenesis in rats. J Comp Neurol. 1965; 124:319–335. [PubMed: 5861717]
5. Kempermann G, Gage FH. Neurogenesis in the adult hippocampus. Novartis Found Symp. 2000; 231:220–235. [PubMed: 11131541]
6. Frederiksen K, McKay RD. Proliferation and differentiation of rat neuroepithelial precursor cells in vivo. J Neurosci. 1988; 8:1144–1151. [PubMed: 3357014]

7. Fukuda S, Kato F, Tozuka Y, Yamaguchi M, Miyamoto Y, Hisatsune T. Two distinct subpopulations of nestin-positive cells in adult mouse dentate gyrus. *J Neurosci*. 2003; 23:9357–9366. [PubMed: 14561863]
8. Kunze A, Grass S, Witte OW, Yamaguchi M, Kempermann G, Redecker C. Proliferative response of distinct hippocampal progenitor cell populations after cortical infarcts in the adult brain. *Neurobiol Dis*. 2006; 21:324–332. [PubMed: 16137890]
9. Brown J, Cooper-Kuhn CM, Kempermann G, Van Praag H, Winkler J, Gage FH, Kuhn HG. Enriched environment and physical activity stimulate hippocampal but not olfactory bulb neurogenesis. *Eur J Neurosci*. 2003; 17:2042–2046. [PubMed: 12786970]
10. Miles DK, Kernie SG. Hypoxic-ischemic brain injury activates early hippocampal stem/progenitor cells to replace vulnerable neuroblasts. *Hippocampus*. 2008; 18:793–806. [PubMed: 18446826]
11. Kernie SG, Erwin TM, Parada LF. Brain remodeling due to neuronal and astrocytic proliferation after controlled cortical injury in mice. *J Neurosci Res*. 2001; 66:317–326. [PubMed: 11746349]
12. Liu L, Cash TP, Jones RG, Keith B, Thompson CB, Simon MC. Hypoxia-induced energy stress regulates mRNA translation and cell growth. *Mol Cell*. 2006; 21:521–531. [PubMed: 16483933]
13. Swiech L, Perycz M, Malik A, Jaworski J. Role of mTOR in physiology and pathology of the nervous system. *Biochim Biophys Acta*. 2008; 1784:116–132. [PubMed: 17913600]
14. Jaworski J, Spangler S, Seeburg DP, Hoogenraad CC, Sheng M. Control of dendritic arborization by the phosphoinositide-3'-kinase-Akt-mammalian target of rapamycin pathway. *J Neurosci*. 2005; 25:11300–11312. [PubMed: 16339025]
15. Kumar V, Zhang MX, Swank MW, Kunz J, Wu GY. Regulation of dendritic morphogenesis by Ras-PI3K-Akt-mTOR and Ras-MAPK signaling pathways. *J Neurosci*. 2005; 25:11288–11299. [PubMed: 16339024]
16. Pei JJ, Hugon J. mTOR-dependent signalling in Alzheimer's disease. *J Cell Mol Med*. 2008; 12:2525–2532. [PubMed: 19210753]
17. Sarkar S, Rubinsztein DC. Huntington's disease: degradation of mutant huntingtin by autophagy. *FEBS J*. 2008; 275:4263–4270. [PubMed: 18637946]
18. Klann E. Thwarting dyskinesia by targeting mTORC1. *Sci Signal*. 2009; 2:pe42. [PubMed: 19622830]
19. Yu TS, Dandekar M, Monteggia LM, Parada LF, Kernie SG. Temporally regulated expression of Cre recombinase in neural stem cells. *Genesis*. 2005; 41:147–153. [PubMed: 15789426]
20. Gilley JA, Yang CP, Kernie SG. Developmental profiling of postnatal dentate gyrus progenitors provides evidence for dynamic cell-autonomous regulation. *Hippocampus*. 2011; 21:33–47. [PubMed: 20014381]
21. Bass JL, Corwin M, Gozal D, Moore C, Nishida H, Parker S, Schonwald A, Wilker RE, Stehle S, Kinane TB. The effect of chronic or intermittent hypoxia on cognition in childhood: a review of the evidence. *Pediatrics*. 2004; 114:805–816. [PubMed: 15342857]
22. Pichiule P, Chavez JC, Boero J, Arregui A. Chronic hypoxia induces modification of the N-methyl-D-aspartate receptor in rat brain. *Neurosci Lett*. 1996; 218:83–86. [PubMed: 8945733]
23. Schlessinger AR, Cowan WM, Gottlieb DI. An autoradiographic study of the time of origin and the pattern of granule cell migration in the dentate gyrus of the rat. *J Comp Neurol*. 1975; 159:149–175. [PubMed: 1112911]
24. Ivasenko IN, Klestova OV, Arkad'eva GE, Almazov VA. Role of stromal microenvironment in the regulation of bone marrow hemopoiesis after curantyl administration. *Biull Eksp Biol Med*. 1990; 110:98–100. [PubMed: 2224116]
25. Tang SJ, Reis G, Kang H, Gingras AC, Sonenberg N, Schuman EM. A rapamycin-sensitive signaling pathway contributes to long-term synaptic plasticity in the hippocampus. *Proc Natl Acad Sci USA*. 2002; 99:467–472. [PubMed: 11756682]
26. Han J, Wang B, Xiao Z, Gao Y, Zhao Y, Zhang J, Chen B, Wang X, Dai J. Mammalian target of rapamycin (mTOR) is involved in the neuronal differentiation of neural progenitors induced by insulin. *Mol Cell Neurosci*. 2008; 39:118–124. [PubMed: 18620060]
27. Corsini NS, Sancho-Martinez I, Laudenklos S, Glasgow D, Kumar S, Letellier E, Koch P, Teodorczyk M, Kleber S, Klussmann S, Wiestler B, Brustle O, Mueller W, Gieffers C, Hill O, Thiemann M, Seedorf M, Gretz N, Sprengel R, Celikel T, Martin-Villalba A. The death receptor

- CD95 activates adult neural stem cells for working memory formation and brain repair. *Cell Stem Cell*. 2009; 5:178–190. [PubMed: 19664992]
28. Zeng LH, Rensing NR, Wong M. The mammalian target of rapamycin signaling pathway mediates epileptogenesis in a model of temporal lobe epilepsy. *J Neurosci*. 2009; 29:6964–6972. [PubMed: 19474323]
29. Li G, Pleasure SJ. Ongoing interplay between the neural network and neurogenesis in the adult hippocampus. *Curr Opin Neurobiol*. 2010; 20:126–133. [PubMed: 20079627]

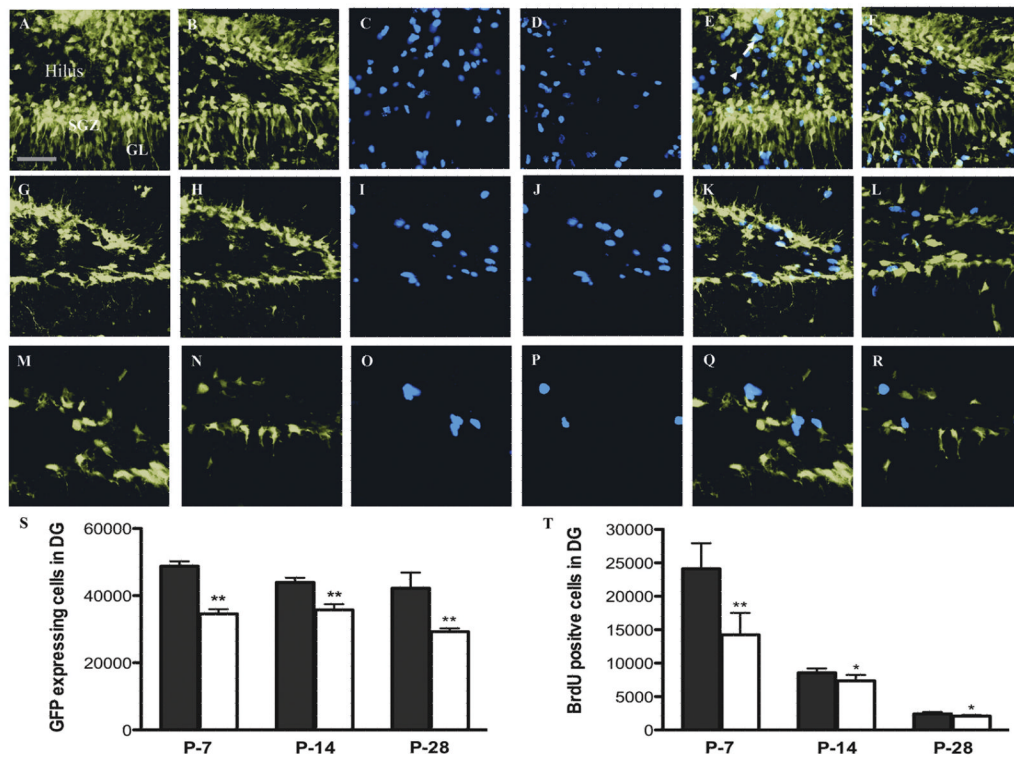


Figure 1. Changes in the progenitor cell population in CH within the dentate gyrus from P7-P28 Representative pictures of GFP and BrdU expression in dentate gyrus (DG) from control *nestin-GFP* mice (P7: A, C; P14: G, I; P28: M, O) and *nestin-GFP* mice exposed to CH (P7: B, D; P14: H, J; P28: N, P) respectively, showing significantly decreased numbers of GFP-positive (S) and BrdU-positive cells (T) in the CH-exposed mice as quantified by design-based stereology. The merged image in the control (P7: E, P-14: K and P28: Q) and CH (P7: F, P14: L, P28: R) shows BrdU-positive cells that are co-localized with GFP (arrows) and BrdU-positive cells that are not (arrowhead). In panels S and T, Control (■) and CH (□). *P*-values for GFP and BrdU are significant. ***P* < 0.001 – 0.01, **P* 0.01 – 0.05 respectively. Error bars represent standard deviation and the scale bar represents 35 μM. GL, granular layer and SGZ, subgranular zone.

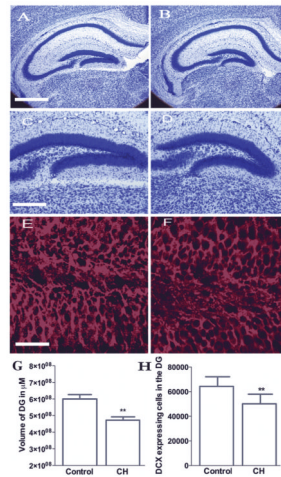


Figure 2. Decreased volume of the dentate gyrus and DCX-expressing late progenitors at P14 following CH

Representative pictures of Nissl staining in control (A and C) and CH (B and D) mice at lower (A and B) and higher magnification (C and D) showing the volume of the DG. Volume estimation by MetaView analysis shows significantly decreased volume in the CH group (G). $**P < 0.001$. Error bars represent standard deviation and scale bars represent 200 μm (A and B) and 100 μm (C and D). Representative pictures of DCX staining in the DG at P14, in the control (E) and CH (F) showing significantly decreased number of cells under CH (H) as quantified by design-based stereology. $**P = 0.001$ to 0.01. Error bars represent standard deviation and scale bars represent 35 μm

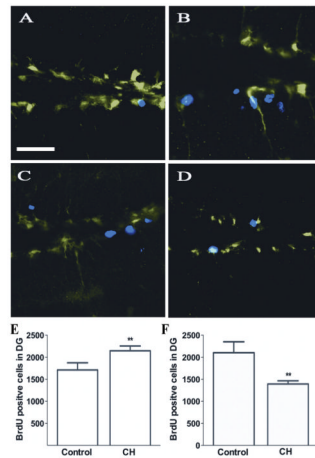


Figure 3. Changes in the number of actively dividing cells within the DG at P56 following CH
 Representative pictures of GFP and BrdU expression in the DG of mice under control (A) and CH conditions (B) shows a significant increase in the number of the BrdU-positive cells in the CH mice (E) as measured by design-based stereology. Mice were injected with BrdU at P28 just after being removed from hypoxic conditions and quantified 4 weeks later. Representative pictures of BrdU staining under control (C) and CH conditions (D) showing decreased number of BrdU-positive cells under CH (F) as measured by design-based stereology. Mice were injected with BrdU 2 hours prior to perfusion at P56. ** $P = 0.001$ to 0.01 . Error bars represent standard deviation and scale bars represent $35 \mu\text{M}$.

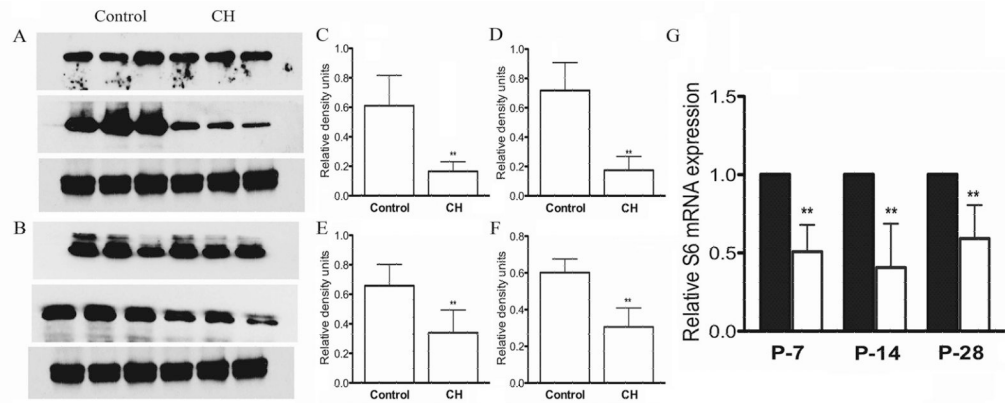


Figure 4. Decreased phosphorylated S6 and 4E-BP1 levels in CH in the cortex

(A) Western blot of total (top) and phosphorylated (p) S6 (middle) showing decreased concentrations of pS6 under CH compared to controls. (B) Western blot of total (top) and phosphorylated (p) 4E-BP1 (middle) showing decreased concentrations of p4E-BP1 in CH compared to the controls. (C) and (D) showing significantly decreased concentrations of pS6 compared to total S6 and tubulin respectively. (E) and (F) show significantly decreased concentrations of p4E-BP1 compared to total 4E-BP1 and tubulin respectively. (G) Significantly decreased expression of S6 mRNA expression is observed at all three time points in the CH group (□) from the FACS-sorted GFP-expressing DG progenitor cells (■). ** $P = 0.001$ to 0.01 and * $P = 0.01 - 0.05$ respectively. Error bars represent standard deviation.

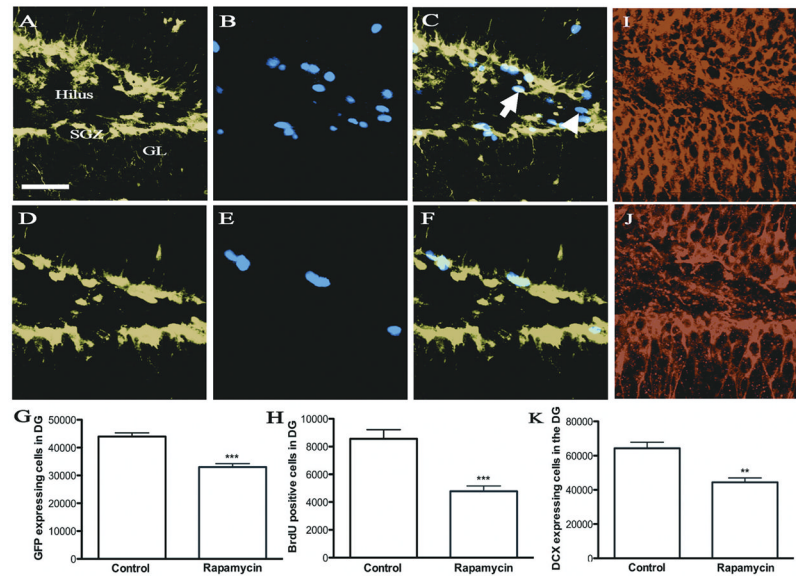


Figure 5. Changes in the progenitor cell population within the DG at P14 following rapamycin injection

Representative pictures of GFP, BrdU and DCX expression in DG from mice under control (A, B, I) and rapamycin-treated conditions (D, E, J) respectively, showing significantly decreased numbers of GFP-positive (G), BrdU-positive cells (H) and DCX-positive cells (K) with rapamycin treatment as quantified by design-based stereology. The merged picture for control (C) and rapamycin treated (F) shows BrdU-positive cells that are co-localized (arrow) and ones that are not (arrowhead). *P*-values for GFP, BrdU and DCX are significant. ***P* < 0.001. Error bars represent standard deviation and scale bars represent 35 μ M.

Table 1

Age	Condition	BrDU (Grid size 100 × 100)		GFP (Grid size 150 × 200)		DCX (Grid size 150 × 200)	
		Average number of cells per sampling site	Coefficient of error	Average number of cells per sampling site	Coefficient of error	Average number of cells per sampling site	Coefficient of error
P-7	Control <i>n</i> = 6	4.5	6%	3.5	8%	NA	NA
	CH <i>n</i> = 6	2.3	8%	3	9.5%		
P-14	Control <i>n</i> = 7	1.5	9.5%	2.5	7.5%	4.5	9.5%
	CH <i>n</i> = 6	1.5	9%	2	11.5%	3.5	7.5%
P-28	Control <i>n</i> = 6	0.5	11%	1.5	6%	NA	NA
	CH <i>n</i> = 7	0.5	9%	1.5	7%		
P-56 (BrDU injected on P28)	Control <i>n</i> = 6	0.5	8%	NA	NA	NA	NA
	CH <i>n</i> = 5	0.5	8%				
P-56 (BrDU injected on P56)	Control <i>n</i> = 5	0.5	10%	NA	NA	NA	NA
	CH <i>n</i> = 5	0.5	10.5%				